SEMARAK ILMU PUBLISHING

Journal of Advanced Research in Fluid Mechanics and Thermal Sciences

Journal homepage:
https://semarakilmu.com.my/journals/index.php/fluid_mechanics_thermal_sciences/index
ISSN: 2289-7879

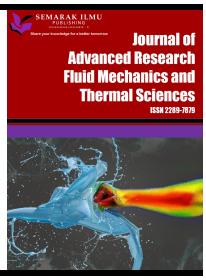

The Influence of Ammonium Formate Concentration on the Electrical Performance of 2-Hydroxyethyl Cellulose Solid Biopolymer Electrolytes

Nur Maisarah Batrisyia Mohd Bahaudin[1], Mohd Ibnu Haikal Ahmad Sohaimy[1], Syahida Suhaimi[3], Wan Mohd Khairul Wan Mohamed Zin[2], Md Uwaisulqarni Osman[2], Mohamad Fakhratul Ridwan Zulkifli[4], Rafizah Rahamathullah[5], Muthuvinayagam Muthiah[6], Mohd Ikmar Nizam Mohamad Isa[1,2,*]

[1] Energy Materials Consortium (EMC), Advanced Materials Team, Ionic & Kinetic Materials Research Laboratory (IKMaR), Faculty of Science & Technology, Universiti Sains Islam Malaysia, 71800 Nilai, Negeri Sembilan Darul Khusus, Malaysia
[2] Advanced Nano Materials (AnoMa), Advanced Materials team, Ionic State Analysis (ISA) Laboratory, Faculty of Science & Marine Environment, Universiti Malaysia Terengganu, 21030 Kuala Nerus, Terengganu Darul Iman, Malaysia
[3] Energy Materials Consortium (EMC), Nano Energy Laboratory (NEL), Faculty of Science & Technology, Universiti Sains Islam Malaysia, 71800 Nilai, Negeri Sembilan Darul Khusus, Malaysia
[4] Marine Materials Research Group, Faculty of Ocean Engineering Technology, Universiti Malaysia Terengganu, 21030 Kuala Nerus, Terengganu Darul Iman, Malaysia
[5] Faculty of Chemical Engineering Technology, Universiti Malaysia Perlis (UniMAP), UniCITI Alam, Sungai Chuchuh, 02100 Padang Besar, Perlis, Malaysia
[6] Department of Applied Physics, Saveetha School of Engineering, Saveetha University (SIMATS), Chennai, India

ARTICLE INFO

Article history:
Received 13 November 2024
Received in revised form 23 April 2025
Accepted 23 August 2025
Available online 22 September 2025

Keywords:
Solid biopolymer electrolyte; ionic conductivity; electrical properties; Rice and Roth

ABSTRACT

Novel solid biopolymer electrolytes (SBE) with various amounts of ammonium formate (AF) salt doped into 2-hydroxyethyl cellulose (2-HEC) are fabricated by using a well-known technique, solution casting. The SBEs are developed mainly to address the leakage, toxic material issues, safety concerns, and costs associated with conventional liquid-based electrolytes. The 2-HEC-based SBE is analyzed for its ionic conductivity and electrical properties. The highest ionic conductivity achieved was 2.40×10^{-3} S/cm for AF40 (40 wt.% AF salt). The bulk resistance value obtained at ambient and elevated temperatures emphasizes its effect on ionic conductivity and electrical behavior regarding its dielectric permittivity. The activation energy from the temperature-dependent ionic conductivity indicates that activation energy decreases with increasing temperature. The two primary transport parameters affecting the system's ionic conductivity based on the Rice and Roth model are the diffusion coefficient (D) and ion mobility (μ). This study showed that the rise in ionic conductivity depends on the concentration of ammonium formate salt.

* *Corresponding author.*
E-mail address: ikmar_isa@usim.edu.my

1. Introduction

Electrolytes are essential in electrochemical systems as they help to facilitate the flow of electric current by dissociating into charged ions. Oxidation and reduction processes occur at the anode and cathode, respectively, and the transfer of chemical compounds involved in these reactions affects the current flow [1,2]. This shows that the electrochemical systems would be unable to function without the presence of electrolytes. Hence, the properties of the electrolyte are a major element to consider in electrochemical systems as it will have a significant impact on the safety, cyclability, rate performance, and energy capacity of all energy storage devices [3,4]. Due to this, researchers are still developing and studying the properties of various types of electrolytes.

Polymer-based electrolyte is one of the electrolyte types used in energy storage that has recently acquired popularity owing to its ability to manufacture flexible and ecologically friendly gadgets [5]. The polymer-based batteries are also said to meet the criteria used in energy storage devices in terms of high performance and cost-effectiveness [6]. Nowadays, the development of polymer electrolytes to solid biopolymer electrolyte (SBE) has been studied by researchers throughout the years. Interest in SBEs in energy storage devices increases mainly due to their biodegradable characteristic in catering the environmental issues. It has been proved that the use of biopolymers obtained from renewable and natural resources for electrochemical applications has been extensively explored over the last two decades. For instance, there are several research focusing on the host polymers of biopolymer electrolytes by using alginate, carboxymethyl cellulose-chitosan, pectin and many more [7-9]. However, polymer-based electrolyte still has drawbacks as most of the pure polymers are classified as a non-conducting substance which result in lower ionic conductivity due to their tendency to easily crystallize [10].

Due to this problem, researchers are finding ways to increase the conductivity value of SBEs. One of the well-known techniques is by adding ionic dopants that will enhance the polymer conductivity due to the capability of mobile ions exchange between the host and salt or weak acid [11,12]. When selecting a doping material, researchers pay attention to the ionic dopants' lattice energy of the materials since it influences the formation of polymer-ionic dopant complexes as proven by Brza *et al.,* [13]. The ion of the dopants will dissolve easily in the matrix polymer and enables the ion dissociation to easily occur if the lattice energy of dopants is low. In this study, ammonium formate salt is used as ionic dopant where the lattice energy reported for AF salt is 737 kJ/mol which can be categorize as suitable to be use as dopant salt [14]. The ammonium salt is reported by researchers as a great ionic dopant for electrolyte and other chemical applications [15]. Based on the research by Muthukrishnan *et al.,* [16], one (1) out of four (4) hydrogen ions, H^+ from ammonium ion, NH_4^+, is loosely attached and easily transfers via hopping mechanism to the coordinating sites in the host polymer which increase the ionic conductivity. In contrast to strong salts or strong acids, ammonium salt – ammonium formate in this proposed study, is a crystalline salt which has high mobility towards the exchange of ions, hence, enhances the conductivity of host polymer.

However, the addition of salt into the polymer does not consistently lead to a proportional increase in conductivity due to some factors, including the nature of the polymer and the specific ions present in the system. Therefore, a study of the impact of ions on salt addition is essential to gain a deeper understanding of the underlying mechanisms. To address this, a detailed investigation using the Rice and Roth model was conducted to comprehend the mechanism of ion transport for achieving optimal ionic conductivity and overall electrolyte performance. The Rice and Roth model clarifies ion conduction in solid biopolymer electrolytes by examining free volume, segmental motion, temperature dependence, and dielectric relaxation subsequently, aiding the future study in electrolytes [17].

In this research, cellulose-based biopolymer, which is 2- Hydroxyethyl Cellulose (2-HEC) is used as the host in the polymer-salt electrolyte system. 2-HEC was selected as host polymer in this study due to its structure which has high ion affinity to act as ion attachments in the system [18]. In addition, 2HEC was reported for its advantages in electrochemical application due to its demand as one of material in battery manufacturing [19]. Thus, this paper investigates the ionic conductivity and electrical properties of 2-HEC/AF electrolyte system where fabricating a biopolymer electrolyte with a good electrical behavior is crucial for electrochemical applications such as in batteries.

2. Methodology

2.1 SBE Preparation

In 100 mL of distilled water, 2 grams of 2-hydroxyethyl cellulose (Sigma Aldrich) were completely dissolved. The 2-HEC solution was then mixed with varying amounts of ammonium formate salts (5 wt.% to 45 wt.%) and continuously stirred with a magnetic stirrer until a homogeneous solution was obtained. The wt.% utilized were ascertain using Eq. (1). The sample designation and composition for 2-HEC/AF were stated in Table 1.

$$AF\ concentration\ (wt.\%) = \frac{mass\ of\ salt\ (g)}{mass\ of\ 2{-}HEC\ (g){+}mass\ of\ salt\ (g)} \times 100 \quad (1)$$

Table 1
List of sample designation and composition for 2-HEC/AF

Sample Designation	AF (wt.%)
AF0	0
AF5	5
AF10	10
AF15	15
AF20	20
AF25	25
AF30	30
AF35	35
AF40	40
AF45	45

For this experiment, a single (1) undoped sample is designated as the control sample. Following that, the homogenous 2-HEC/AF solution was poured into petri dishes and were allowed to dry at room temperature until thin film samples formed. Prior to being subjected to further analysis, the dried thin films were kept in desiccators to maintain the physical properties of the sample. The simplified 2-HEC/AF biofilm fabrication process is depicted in Figure 1, wherein the solution casting technique yielded a transparent, flexible, and free-standing thin film.

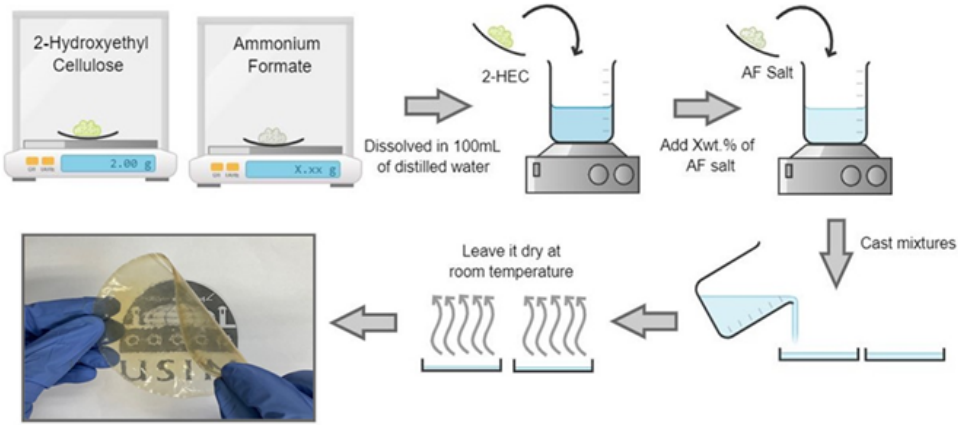

Fig. 1. The fabrication process of 2-HEC/AF biofilm electrolytes

2.2 Characterization of 2-Hydroxyethyl Cellulose Ammonium Formate (2-HEC/AF) Biofilm Electrolytes via Impedance Spectroscopy

The conductivities and dielectric behaviors of 2-HEC/AF were measured by using HIOKI IM 3570-50 LCR Hi-Tester in the frequency range of 50 Hz to 1 MHz. The SBE thin films with thickness ranging from 0.0091 cm to 0.0185 cm were precisely cut into 2.0 cm diameter disks using sharp razor blade. These thin films were then placed between two stainless steel electrodes in the sample holder. The thin film will then undergo electrical testing which facilitates obtaining impedance dataset, in order to study its electrical behavior in terms of ionic conductivity and dielectric characteristics.

3. Results and Discussions

3.1 Ionic Conductivity Analysis

Impedance spectrum for various concentrations of salt starting from AF0 until AF45 with interval of 5wt.% are presented in Figure 2(a) to Figure 2(d). The imaginary impedance component (Z_i) versus the real impedance component (Z_r) that can be observed in the graph is displayed as the Cole–Cole plot, which also referred as the impedance or Nyquist plot. The Cole-Cole plot is used to analyze the electrical behavior of electrolyte in terms of its conductivity, frequency-dependent properties of materials and its relaxation behavior. Based on the graph in Figure 2(a), the spectra show two distinct sections of the spectrum which are semicircles at high frequency region and spike line at low frequency region. The reduction of semicircle in Cole-Cole plot graph can be observed as the addition of salt increasing which affects the bulk resistance value of electrolytes where it drops until AF40. However, the bulk resistance for AF45 start to rise which means that the ionic conductivity drops at the addition of 45wt.% of AF salt. The Impedance test for AF50 was not performed as the sample was physically unstable and had a jelly-like texture, therefore was not used for testing.

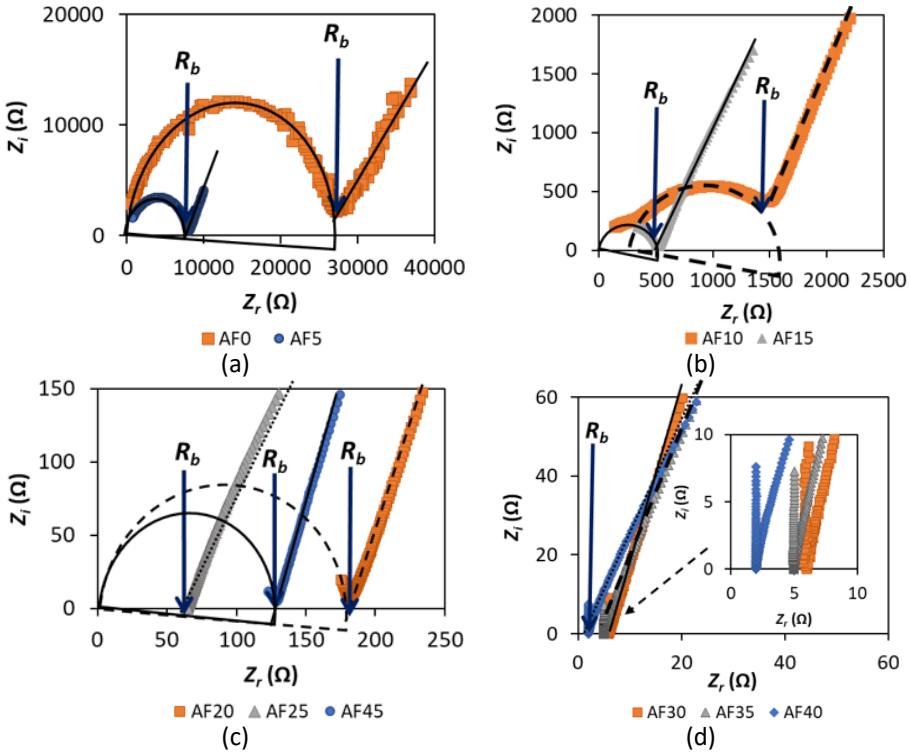

Fig. 2. Cole-Cole plots for 2-HEC/AF samples at 303K

Figure 3 shows the impedance plot for AF40 at higher temperature. The decrease in R_b as temperature increases is due to the rises of thermal energy in the system which aid in the increase of ions mobility. Due to this, ions are able to overcome energy barriers easily hence improving the ionic conductivity of the electrolyte. The increase in ionic conductivity due to the decreases of R_b can be further studied and proved in the temperature dependence studies part which highlights the critical role of temperature in enhancing ion transport in the system. It is noted that other samples also show similar trends in decreases of R_b as temperature increases as shown in Figure 3.

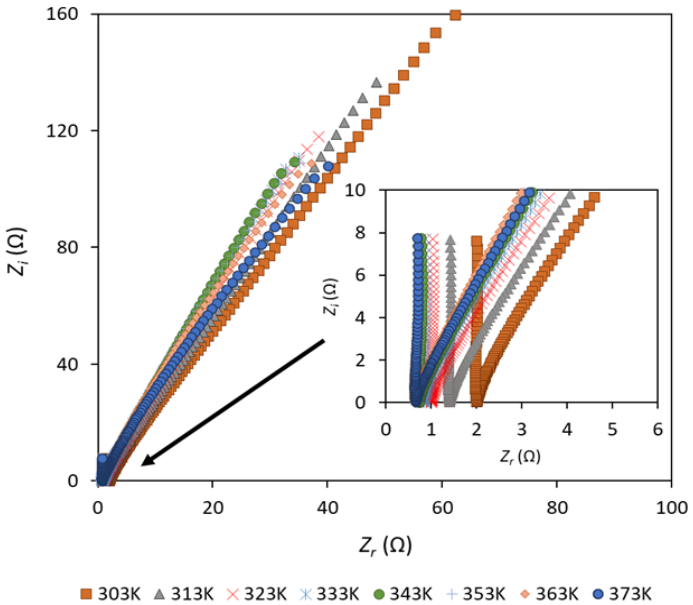

Fig. 3. Cole-Cole plots for AF40 at elevated temperatures (303K – 373K)

The ionic conductivity of each sample was then determined from the bulk resistance (R_b) value using Eq. (2) below

$$\sigma = \frac{t}{R_b \cdot A} \tag{2}$$

where t is thickness of the electrolytes, A is area of electrode-electrolyte (cm^2) and R_b is bulk resistance [20]. The bulk resistance (R_b) is obtained through the analysis of the impedance plot, where the value can be determined from the intersection of high and low frequency. The average ionic conductivity values obtained for each sample at room temperature are plotted in Figure 4 and recorded in Table 2. Based on the graph, it can be observed that the ionic conductivity increases alongside with the addition of AF salt. The ionic conductivity for pure sample, AF0 is 1.590×10^{-7} S/cm while at AF40 sample depicts the highest conductivity value which is 2.400×10^{-3} S/cm. The increases in ionic conductivity of the SBE sample are proved due to the higher charge carrier in the system which leads to increase in ion-pair dissociation and ions mobility [21,22]. However, further addition of salt will lead to the decreases of ionic conductivity as can be seen for AF45. It is due to aggregations of ions in the polymer chain thus hindering the movement of ion [23].

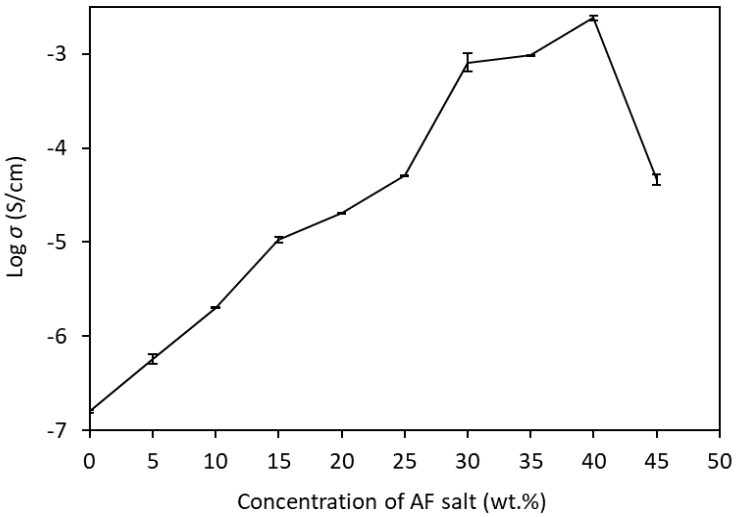

Fig. 4. Ionic conductivity graph for all 2-HEC/AF samples with various concentrations of AF salt

Table 2
Values of ionic conductivity for sample AF0 until AF45 respectively

Sample	Conductivity, σ (S/cm)
AF0	1.590×10^{-7} (±0.008)
AF5	5.730×10^{-7} (±0.041)
AF10	1.997×10^{-6} (±0.026)
AF15	1.060×10^{-5} (±0.533)
AF20	2.021×10^{-5} (±0.250)
AF25	5.114×10^{-5} (±0.494)
AF30	8.090×10^{-4} (±0.146)
AF35	9.710×10^{-4} (±0.001)
AF40	2.400×10^{-3} (±2.740)
AF45	4.580×10^{-5} (±5.304)

3.2 Ionic Conductivity Analysis

The ionic conductivities of SBEs for each sample were further studied at elevated temperatures in the range of 303K to 373K. Figure 5 portrays the temperature dependence graph of log σ against 1000/T for selected samples (AF0, AF10, AF20, AF30 and AF40). The figure shows that as the temperature increases, the conductivity increases linearly. The conductivity increased maybe due to several reasons such as the heat activation of charge carriers which thermally induced the creation of more vacant sites for ion mobility and increase the free volume of ions [24]. Table 3 presents the R^2 values for each sample with varied concentration of AF salt at elevated temperatures which shows that the system exhibits the Arrhenius behavior where the regression value is below or near to unity, $R^2 \approx 1$ [25].

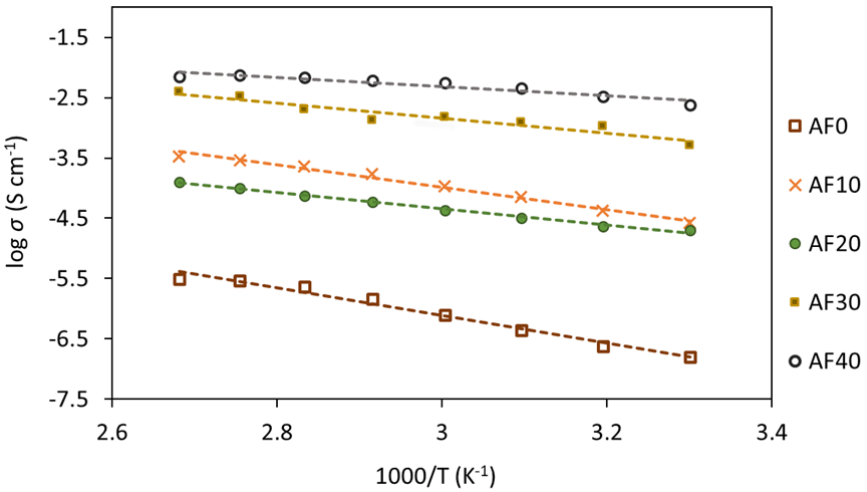

Fig. 5. The Arrhenius plot for 2-HEC/AF samples at elevated temperatures (303K – 373K)

Table 3
Regression, R^2 and activation energy, E_a values of 2-HEC/AF samples

Sample	Regression value R^2 (Ω)	Activation energy E_a (eV)
AF0	0.98	0.20
AF10	0.99	0.16
AF20	0.99	0.12
AF30	0.91	0.11
AF40	0.90	0.07

The activation energy, E_a was obtained through the linear fit data of temperature dependence plot by using Eq. (3), where E_a is the activation energy, σ is the conductivity of samples, σ_0 is the pre-exponential factor, k is Boltzmann constant, and T is the temperature (Kelvin). The kinetics of ionic diffusion for 2-HEC/AF samples can be compared using activation energy obtained from the temperature dependence plot. Figure 6 shows the plot of activation energy versus concentration of AF salt and the values are tabulated in Table 3. It can be seen from the figure that the lower the activation energy of samples, the higher the ionic conductivity of the samples. Therefore, the decrease in E_a value will lead to higher ionic conductivity of samples, indicating that the H^+ ions only need a small amount of energy to promotes ionic mobility and diffusion within the polymer's backbone to increase ionic conductivity [26].

$$\sigma = \sigma_o exp \frac{-E_a}{k_B T} \quad (3)$$

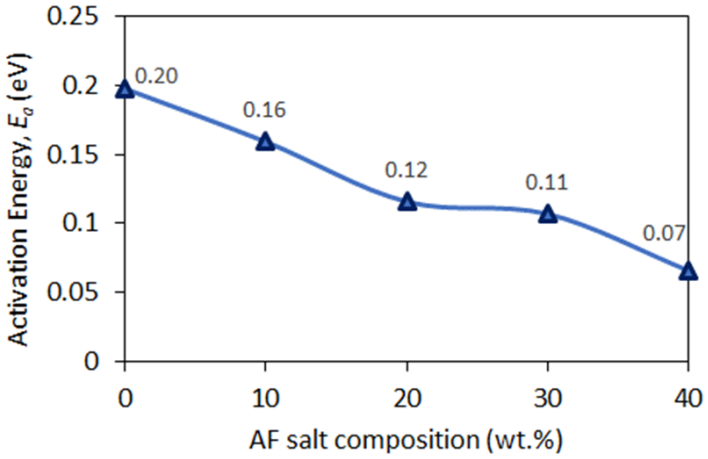

Fig. 6. Graph of activation energy, E_a against concentration of AF salt

3.3 Dielectric Study Analysis

The conductivity behavior of the biopolymer electrolytes was further examined through dielectric studies which determine the molecular behavior of the polymer electrolytes. The dielectric studies investigated the storage of charges and energy loss during the movement of the ions inside the electrolytes which are represented by the real part of dielectric constant (ε_r) and imaginary part of dielectric constant (ε_i), respectively [27]. The real part (ε_r) and imaginary part (ε_i) were calculated using Eq. (4) and Eq. (5), where $C_0 = \frac{\varepsilon_0 A}{t}$, $\varepsilon_0 = 8.55 \times 10^{-12}$ Fm^{-1}, $\omega = 2\pi f$.

$$\varepsilon_r(\omega) = \frac{Z_i}{\omega C_o (Z_r{}^2 + Z_i{}^2)} \quad (4)$$

$$\varepsilon_i(\omega) = \frac{Z_r}{\omega C_o (Z_r{}^2 + Z_i{}^2)} \quad (5)$$

The frequency dependence for ε_r and ε_i of 2-HEC/AF samples at different temperatures is plotted as shown in Figure 7 and Figure 8 respectively. The common pattern shown in the figures is that the dielectric permittivity is inversely proportional with the frequency where the dielectric permittivity decreases as frequencies increases. Based on both graph for ε_r and ε_i, the plot can be generally classified into two parts where at low frequency, the significant increase in dielectric permittivity indicates the effects of electrode polarization due to the occurrence of space charge [28]. Meanwhile at high frequency, the reversal of electric field occurred rapidly, which prevented more ions diffusing in either direction of the field, thus leading to reduction in dielectric permittivity [29]. The presence of hump in the graph of ε_i can be attributed as occurrence of structural relaxation process where the rearrangements of molecules in polymer chains become more active and has reach its maximum intensity which enhanced the ion mobility in system [30]. It also can be observed that both ε_r and ε_i increase along with the increase in temperature. The thermal energy supplied to the electrolyte system allows the ions to diffuse more within the host polymer as it can easily overcome intermolecular forces and energy barriers at elevated temperatures. Thus, the dissociation of AF salt

into NH_4^+ and $HCOO^-$ ions will also increase resulting in higher density of charge carriers within the polymer electrolyte which aid in enhanced the ionic conductivity.

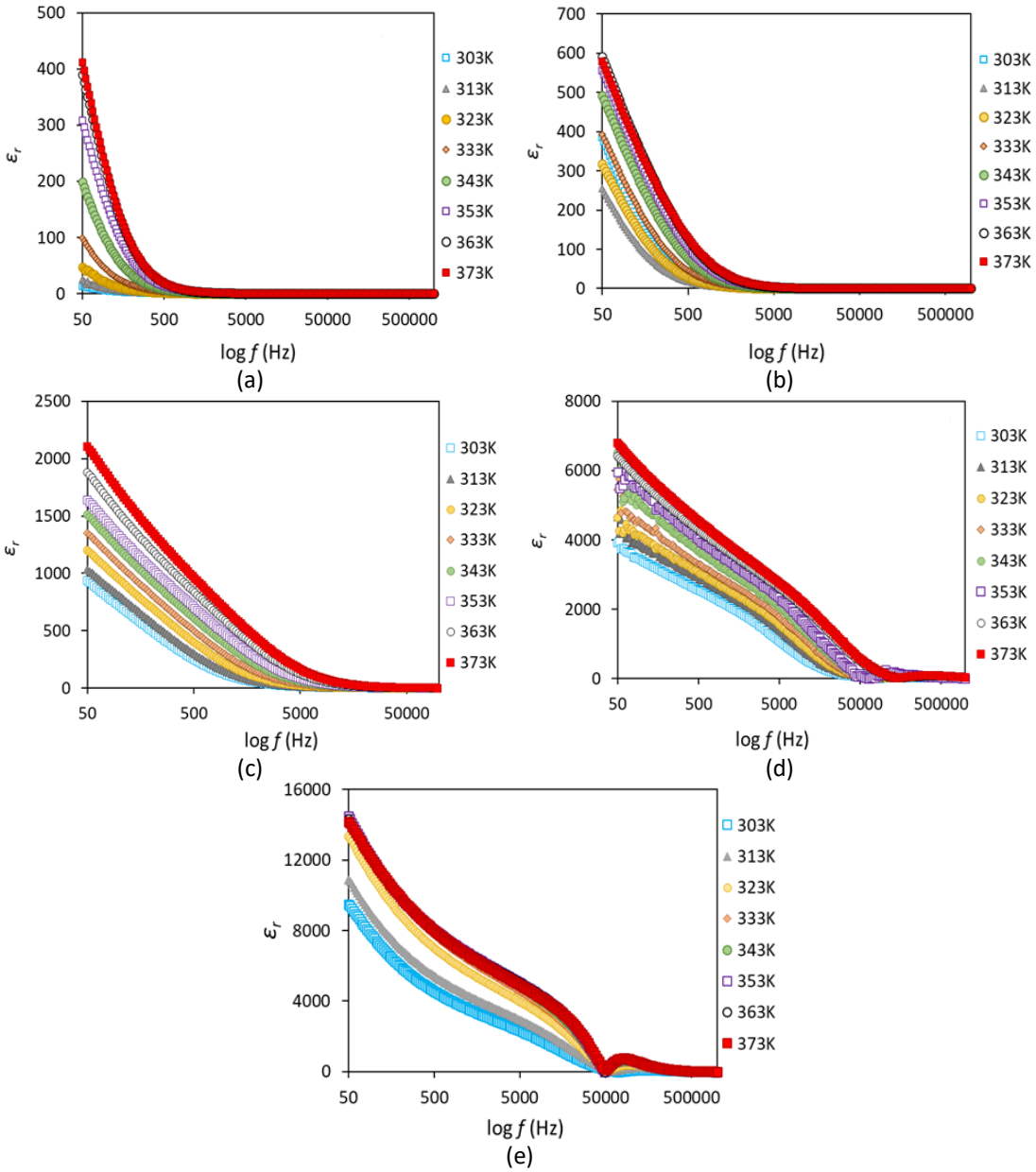

Fig. 7. Frequency dependence of ε_r for (a) AF0, (b) AF10, (c) AF20, (d) AF30, and (e) AF40 at different temperatures

The dielectric behavior for SBEs samples is further studies through the electrical modulus. The equations for real part (M_r) and imaginary part (M_i) of electrical modulus can be calculated from the dielectric permittivity using the following Eq. (6) and Eq. (7);

$$M_r(\omega) = \frac{\varepsilon_r}{(\varepsilon_r{}^2 + \varepsilon_i{}^2)} \tag{6}$$

$$M_i(\omega) = \frac{\varepsilon_i}{(\varepsilon_r{}^2 + \varepsilon_i{}^2)} \tag{7}$$

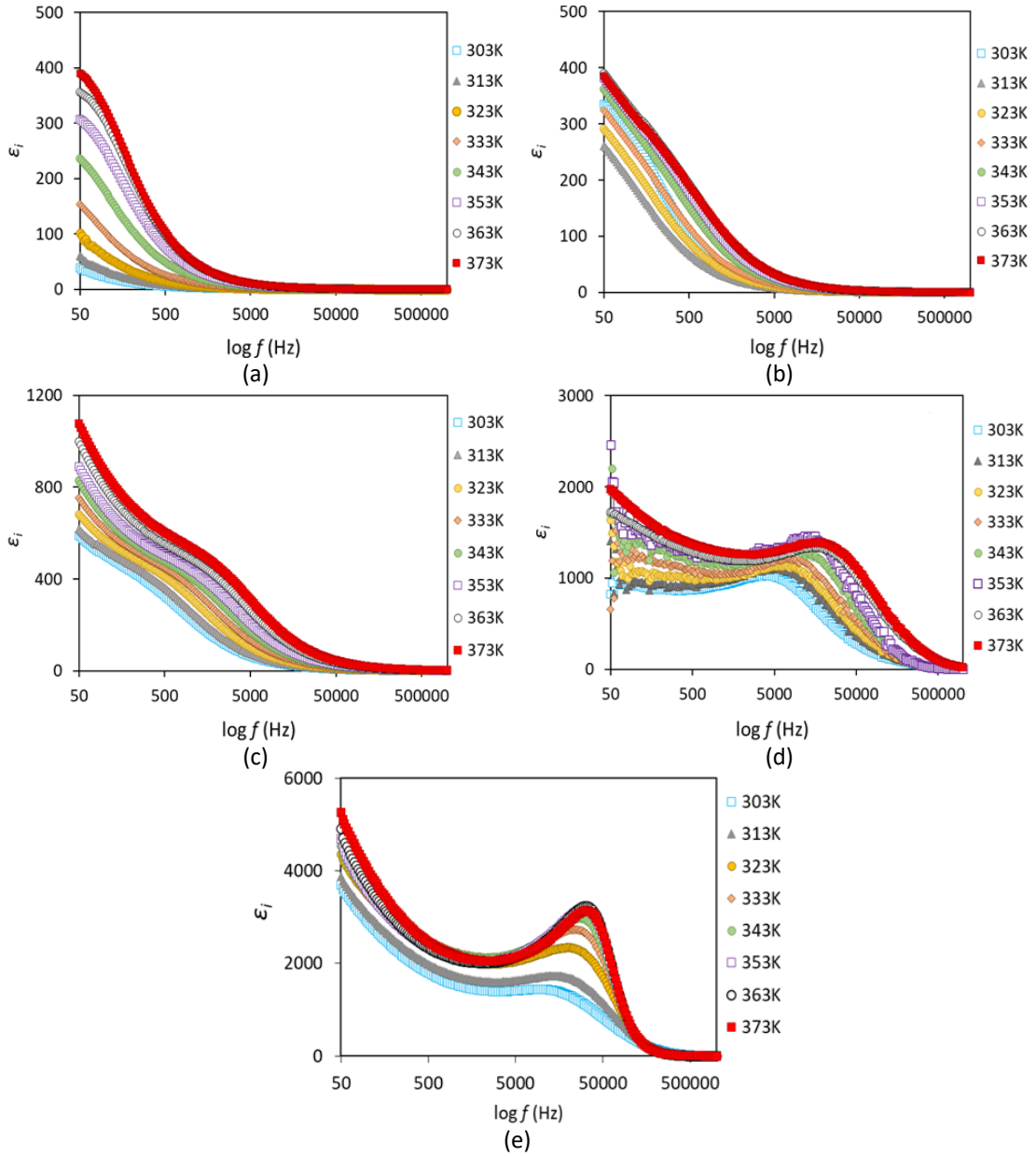

Fig. 8. Frequency dependence of ε_i for (a) AF0, (b) AF10, (c) AF20, (d) AF30, and (e) AF40 at different temperatures

Figure 9 and Figure 10 depicts the real part of electrical modulus (M_r) and the imaginary part of electrical modulus (M_i) against frequency for selected samples of 2-HEC/AF (AF0, AF10, AF20, AF30 and AF40) at elevated temperature respectively. Based on the figure in the plot of M_r and M_i, the lengthy tail seen at the lower frequency is mostly attributed to the suppression of the electrode polarization (EP) effect involved in the electrical modulus study [24]. This observation of the long tail at M_r and M_i is supported by the high value of the dielectric constant at low frequencies as seen in Figure 7 and Figure 8. Besides, it can be observed that the curve for both M_r and M_i shifted towards the right side of higher frequencies with an increase in temperature. The shift of the curves alongside the decrease in modulus value for M_r and M_i are due to the increase in temperature which lead to shorter rate of relaxation process thus improved the mobility of ion and conductivity [31]. From this study, it can be concluded that as the temperature increases, the relaxation time decreases leading to an increase in ion mobility and ionic conductivity of the system.

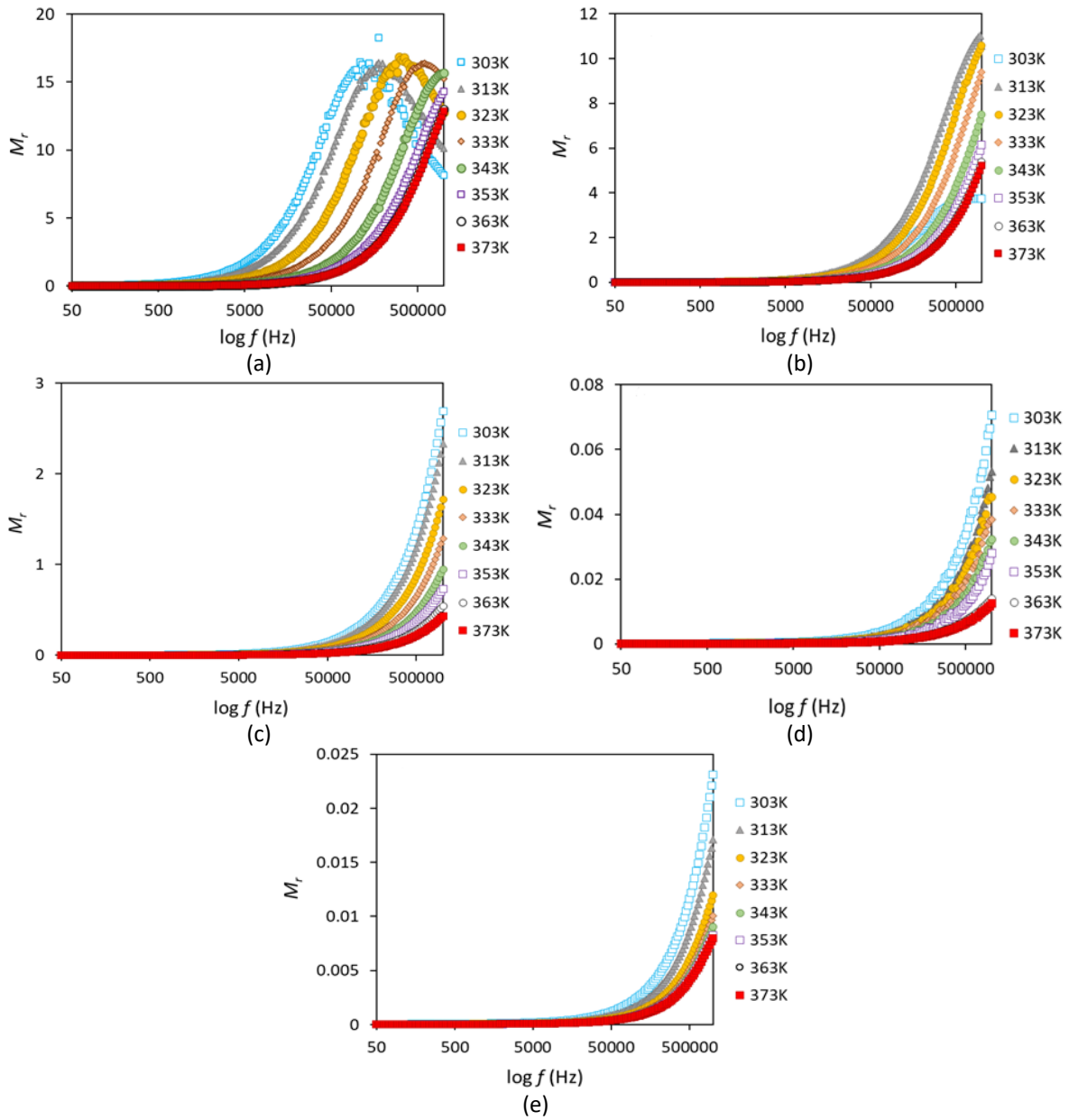

Fig. 9. Frequency dependence of M_r for (a) AF0, (b) AF10, (c) AF20, (d) AF30, and (e) AF40 at elevated temperatures

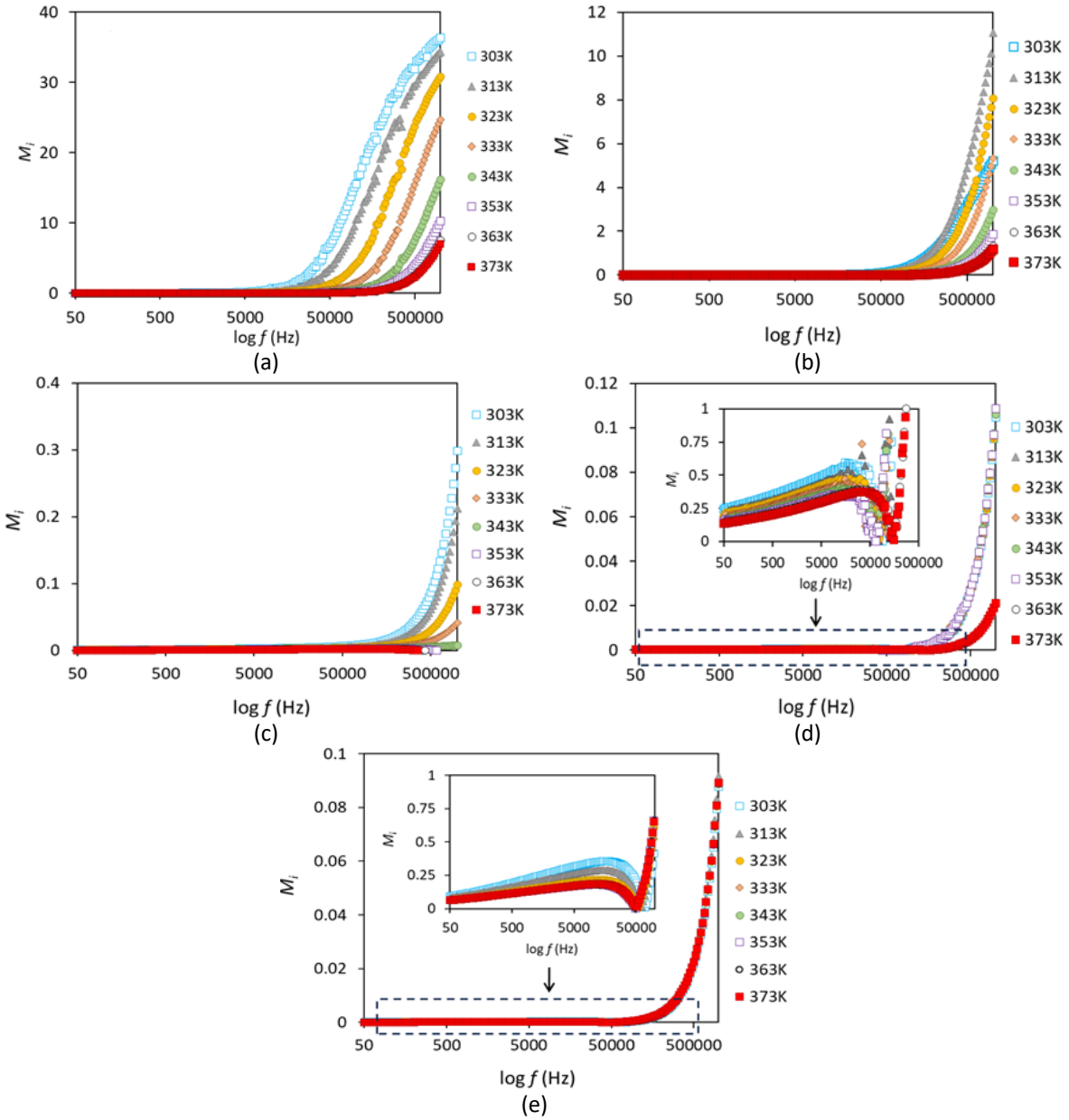

Fig. 10. Frequency dependence of M_i for (a) AF0, (b) AF10, (c) AF20, (d) AF30, and (e) AF40 at elevated temperatures

3.4 Ion Transport Parameters Analysis

A study on transport parameters was carried out in order to determine the system's diffusion coefficient (D), ion mobility (μ), and total number of mobile ions (η). The Rice and Roth model is used to measure the transport parameters in the polymer electrolyte based on the collected data of impedance spectroscopy. Rice and Roth were chosen because the system obeyed the Arrhenius law, where conductivity increases as temperature increases [32]. Based on Rice and Roth model, energy gap exists in the electrolyte where ions with mass, m, at ionic states are thermally excited to free-ion states where the velocity required for the movement of ions can be calculated using Eq. (6), where E_a is activation energy and m is the mass of proton. The ionic conductivity from Rice-Roth model in Eq. (7) was derived to be used in calculating the number of mobile ions (η) by using Eq. (8), where T is ambient temperature, e is the electric charge and τ is finite lifetime.

$$v = \sqrt{\frac{2(E_a)}{m}} \tag{6}$$

$$\sigma = \frac{1}{3}\left[\frac{(Ze)^2}{k_B T}\right][nlv]\left[\exp\left(-\frac{E_a}{k_B T}\right)\right] \tag{7}$$

$$\eta = \frac{3\sigma kTm}{2e^2 E_a \tau e^{\left(-\frac{E_a}{kT}\right)}} \tag{8}$$

To determine the finite lifetime of the excited free ion based on Eq. (9), the distance between the coordinating sites where hopping of ions occurs (*l*) must be attained where the value of *l* for cellulose fibril is generally at 1.5nm [33]. The diffusion coefficient of ions (*D*) and the mobility of ions (μ) are calculated by using Eq. (10) and Eq. (11) respectively.

$$\tau = \frac{l}{v} \tag{9}$$

$$\mu = \frac{\sigma}{ne} \tag{10}$$

$$D = \frac{k_B T \sigma}{ne^2} \tag{11}$$

The values of the transport parameters in relation to the composition of AF salt are obtained and tabulated in Table 4. Based on the data tabulated, it can be observed η values increases alongside with the addition of AF salt. However, AF30 shows the highest value of η although it is not the highest conducting sample. It can be observed that there is a slight decrease in number of mobile ions at AF40 due to the ions starting to aggregate. However, the μ and *D* value shows different pattern where both value increases at AF40 substantially increases in contrast to the decrease value of η. This behavior suggests the possibility of an ion pathway existing through the polymer segmental motion in the SBE which creates a route for the ions to move in the system. Based on Figure 4, the ionic conductivity improvement at AF30 occurred at a higher rate compared to the rest samples. This also coincides with the huge increase of η at AF30. The continued rise of ionic conductivity at AF40 is believed to be due to longer formation of polymer segmental motion as the increases of salt disrupt the hydrogen bonding in polymer chains more [34]. The elongation of polymer segmental motion aids in efficiency of the ions movement by providing longer pathway for ions despite the aggregation that occurred. Thus, the presence of the pathway in AF40 improved the mobility of ions and diffusion coefficient which increase the ionic conductivity of the sample. Concisely, the ionic conductivity of 2-HEC/AF depends on the mobility of ions (μ) and diffusion coefficients (*D*).

Table 4
The transport parameters for 2-HEC/AF samples

Sample	$\sigma \times 10^{-5}$ (Scm^{-1})	$\tau \times 10^{-22}$ (s)	$\eta \times 10^{30}$ (cm^{-3})	$\mu \times 10^{-15}$ ($cm^2 V^{-1} s^{-1}$)	$D \times 10^{-22}$ ($cm^2 s^{-1}$)
AF0	0.02	0.97	0.04	0.02	0.01
AF10	0.20	1.09	0.13	0.09	0.05
AF20	2.02	1.27	0.30	0.42	0.29
AF30	80.90	1.32	8.85	0.57	0.41
AF40	240.00	1.69	6.92	2.17	1.97

4. Conclusions

In conclusion, the objectives for this study are successfully achieved where the 2-HEC/AF thin film was fabricated through the solution casting. The SBEs appeared to have a transparent physical appearance and behaved like plastic behavior. The ionic conductivity of 2-HEC/AF samples improves alongside the addition of AF salt until it reached 40 wt.% of AF salt where it achieved the highest conductivity at 2.40×10^{-3} S/cm. At elevated temperature, the ionic conductivity of 2-HEC/AF samples are proved to be increase linearly. The result obtained shows that SBE samples obeyed the Arrhenius rules in term of regression value and the conductivity increases as the temperature increases. The constant rise in conductivity mainly caused by the mobility of ions (μ) and diffusion coefficients (D) due to the presence of percolation network which create more pathways for ionic transport. Hence, influenced the increase of ionic conductivity of samples. Nonetheless, further study needs to be done to improve the ionic conductivity and the physical behavior of the electrolyte by adding plasticizers or fillers to the system.

Acknowledgement

This work was financially supported by Universiti Sains Islam Malaysia under Grant PPPI/PENTADBIR/FST/USIM/19123.

References

[1] Galle Kankanamge, Susith R., and Daniel G. Kuroda. "Molecular structure, chemical exchange, and conductivity mechanism of high concentration LiTFSI electrolytes." *The Journal of Physical Chemistry B* 124, no. 10 (2020): 1965-1977. https://doi.org/10.1021/acs.jpcb.9b10795

[2] Ilic, Ivan K., Valerio Galli, Leonardo Lamanna, Pietro Cataldi, Lea Pasquale, Valerio F. Annese, Athanassia Athanassiou, and Mario Caironi. "An edible rechargeable battery." *Advanced Materials* 35, no. 20 (2023): 2211400. https://doi.org/10.1002/adma.202211400

[3] Karuppasamy, K., Jayaraman Theerthagiri, Dhanasekaran Vikraman, Chang-Joo Yim, Sajjad Hussain, Ramakant Sharma, Thandavaryan Maiyalagan, Jiaqian Qin, and Hyun-Seok Kim. "Ionic liquid-based electrolytes for energy storage devices: A brief review on their limits and applications." *Polymers* 12, no. 4 (2020): 918. https://doi.org/10.3390/polym12040918

[4] Meng, Y. Shirley, Venkat Srinivasan, and Kang Xu. "Designing better electrolytes." *Science* 378, no. 6624 (2022). https://doi.org/10.1126/science.abq3750

[5] Dennis, John Ojur, M. F. Shukur, Osamah A. Aldaghri, Khalid Hassan Ibnaouf, Abdullahi Abbas Adam, Fahad Usman, Yarima Mudassir Hassan, A. Alsadig, Wilson L. Danbature, and Bashir Abubakar Abdulkadir. "A review of current trends on polyvinyl alcohol (PVA)-based solid polymer electrolytes." *Molecules* 28, no. 4 (2023): 1781. https://doi.org/10.3390/molecules28041781

[6] Ghazali, Nuraziliana Muhd, and Ahmad Salihin Samsudin. "Progress on biopolymer as an application in electrolytes system: A review study." *Materials Today: Proceedings* 49 (2022): 3668-3678. https://doi.org/10.1016/j.matpr.2021.09.473

[7] Fuzlin, A. F., M. A. Saadiah, Md M. Hasan, Y. Nagao, I. I. Misnon, and A. S. Samsudin. "Involvement of ethylene carbonate on the enhancement H^+ carriers in structural and ionic conduction performance on alginate bio-based polymer electrolytes." *International Journal of Hydrogen Energy* 47, no. 12 (2022): 7846-7860. https://doi.org/10.1016/j.ijhydene.2021.12.124

[8] Helen, P. Adlin, K. Ajith, M. Infanta Diana, D. Lakshmi, and P. Christopher Selvin. "Chitosan based biopolymer electrolyte reinforced with V_2O_5 filler for magnesium batteries: an inclusive investigation." *Journal of Materials Science: Materials in Electronics* 33, no. 7 (2022): 3925-3937. https://doi.org/10.1007/s10854-021-07587-7

[9] Mohapatra, Sipra, Hema Teherpuria, Sapta Sindhu Paul Chowdhury, Suleman Jalilahmad Ansari, Prabhat K. Jaiswal, Roland R. Netz, and Santosh Mogurampelly. "Ion transport mechanisms in pectin-containing EC-LiTFSI electrolytes." *Nanoscale* 16, no. 6 (2024): 3144-3159. https://doi.org/10.1039/D3NR04029A

[10] Reddy, P. C. Himadri, John Amalraj, S. Ranganatha, Smitha S. Patil, and Saravanan Chandrasekaran. "A review on effect of conducting polymers on carbon-based electrode materials for electrochemical supercapacitors." *Synthetic Metals* 298 (2023): 117447. https://doi.org/10.1016/j.synthmet.2023.117447

[11] Jacobs, Ian E., Gabriele d'Avino, Vincent Lemaur, Yue Lin, Yuxuan Huang, Chen Chen, Thomas F. Harrelson et al. "Structural and dynamic disorder, not ionic trapping, controls charge transport in highly doped conducting polymers." *Journal of the American Chemical Society* 144, no. 7 (2022): 3005-3019. https://doi.org/10.1021/jacs.1c10651

[12] Sagar, Rohan Nandeesh, Ravindrachary Vasachar, and Shreedatta Hegde. "Microstructure and electrical properties of Li^+ ion conducting polymer blend electrolyte films." *Express Polymer Letters* 17, no. 9 (2023). https://doi.org/10.3144/expresspolymlett.2023.66

[13] Brza, Mohamad A., Shujahadeen B. Aziz, Muaffaq M. Nofal, Salah R. Saeed, Shakhawan Al-Zangana, Wrya O. Karim, Sarkawt A. Hussen, Rebar T. Abdulwahid, and Mohd F. Z. Kadir. "Drawbacks of low lattice energy ammonium salts for ion-conducting polymer electrolyte preparation: structural, morphological and electrical characteristics of CS: PEO: NH_4BF_4-based polymer blend electrolytes." *Polymers* 12, no. 9 (2020): 1885. https://doi.org/10.3390/polym12091885

[14] Sohaimy, M. I. H., and M. I. N. Isa. "Proton-conducting biopolymer electrolytes based on carboxymethyl cellulose doped with ammonium formate." *Polymers* 14, no. 15 (2022): 3019. https://doi.org/10.3390/polym14153019

[15] Nofal, Muaffaq M., Shujahadeen B. Aziz, Mohamad A. Brza, Sozan N. Abdullah, Elham M. A. Dannoun, Jihad M. Hadi, Ary R. Murad, Sameerah I. Al-Saeedi, and Mohd F. Z. Kadir. "Studies of circuit design, structural, relaxation and potential stability of polymer blend electrolyte membranes based on PVA: MC impregnated with NH_4I salt." *Membranes* 12, no. 3 (2022): 284. https://doi.org/10.3390/membranes12030284

[16] Muthukrishnan, M., C. Shanthi, S. Selvasekarapandian, G. Shanthi, L. Sampathkumar, and T. Maheshwari. "Impact of ammonium formate (AF) and ethylene carbonate (EC) on the structural, electrical, transport and electrochemical properties of pectin-based biopolymer membranes." *Ionics* 27, no. 8 (2021): 3443-3459. https://doi.org/10.1007/s11581-021-04106-w

[17] Ahmed, Mohammed B., Shujahadeen B. Aziz, and Ary R. Murad. "Diffusion and ion carrier mobility studies in binary SPEs based on PVA integrated with K^+ ion provider salt: structural and electrical insights." *Ionics* 28, no. 11 (2022): 5153-5169. https://doi.org/10.1007/s11581-022-04728-8

[18] Rayung, Marwah, Min Min Aung, Shah Christirani Azhar, Luqman Chuah Abdullah, Mohd Sukor Su'ait, Azizan Ahmad, and Siti Nurul Ain Md Jamil. "Bio-based polymer electrolytes for electrochemical devices: Insight into the ionic conductivity performance." *Materials* 13, no. 4 (2020): 838. https://doi.org/10.3390/ma13040838

[19] Mejenom, Amzar Arif, Muthuvinayagam Muthiah, and Mohd Ikmar Nizam Mohamad Isa. "Ionic Conductivity Studies on Proton Conducting Solid Biopolymer Electrolyte based on 2-Hydroxyethyl Cellulose (2HEC) Doped with Ammonium Chloride (NH_4CL)." *Journal of Advanced Research in Fluid Mechanics and Thermal Sciences* 121, no. 2 (2024): 147-158. https://doi.org/10.37934/arfmts.121.2.147158

[20] Hama, Peshawa O., M. A. Brza, Hawzhin B. Tahir, Shujahadeen B. Aziz, Bandar Ali Al-Asbahi, and Abdullah Ahmed Ali Ahmed. "Simulated EIS and Trukhan model to study the ion transport parameters associated with Li+ ion dynamics in CS based polymer blends inserted with lithium nitrate salt." *Results in Physics* 46 (2023): 106262. https://doi.org/10.1016/j.rinp.2023.106262

[21] Li, Zhuo, Jialong Fu, Xiaoyan Zhou, Siwei Gui, Lu Wei, Hui Yang, Hong Li, and Xin Guo. "Ionic conduction in polymer-based solid electrolytes." *Advanced Science* 10, no. 10 (2023): 2201718. https://doi.org/10.1002/advs.202201718

[22] Zhang, Dongmei, Xianglong Meng, Wenyan Hou, Weihao Hu, Jinshan Mo, Tianrong Yang, Wendi Zhang et al. "Solid polymer electrolytes: Ion conduction mechanisms and enhancement strategies." *Nano Research Energy* 2, no. 2 (2023): e9120050. https://doi.org/10.26599/NRE.2023.9120050

[23] Bakar, Recep, Saeid Darvishi, Umut Aydemir, Ugur Yahsi, Cumali Tav, Yusuf Ziya Menceloglu, and Erkan Senses. "Decoding polymer architecture effect on ion clustering, chain dynamics, and ionic conductivity in polymer electrolytes." *ACS Applied Energy Materials* 6, no. 7 (2023): 4053-4064. https://doi.org/10.1021/acsaem.3c00310

[24] Ratri, Christin Rina, Qolby Sabrina, Titik Lestariningsih, Adam Febriyanto Nugraha, Sotya Astutiningsih, and Mochamad Chalid. "Unveiling frequency-dependent dielectric behavior of cellulose-based polymer electrolyte at various temperature and salt concentration." *International Journal of Renewable Energy Development* 12, no. 4 (2023). https://doi.org/10.14710/ijred.2023.53103

[25] Taira, Kenji, Daniel McInnes, and Lian Zhang. "How many data points and how large an R-squared value is essential for Arrhenius plots?." *Journal of Catalysis* 419 (2023): 26-36. https://doi.org/10.1016/j.jcat.2023.01.033

[26] Zhu, Lei, Youwei Wang, Junchao Chen, Wenlei Li, Tiantian Wang, Jie Wu, Songyi Han et al. "Enhancing ionic conductivity in solid electrolyte by relocating diffusion ions to under-coordination sites." *Science Advances* 8, no. 11 (2022). https://doi.org/10.1126/sciadv.abj7698

[27] Adam, Abdullahi Abbas, Hassan Soleimani, John Ojur Dennis, Osamah A. Aldaghri, Ahmed Alsadig, Khalid Hassan Ibnaouf, Bashir Abubakar Abdulkadir, Ismael Abdalla Wadi, Vipin Cyriac, and Muhammad Fadhlullah Bin Abd Shukur. "Insight into the effect of glycerol on dielectric relaxation and transport properties of potassium-ion-

conducting solid biopolymer electrolytes for application in solid-state electrochemical double-layer capacitor." *Molecules* 28, no. 8 (2023): 3461. https://doi.org/10.3390/molecules28083461

[28] Qiu, Jie, Qun Gu, Ye Sha, Yang Huang, Meng Zhang, and Zhenyang Luo. "Preparation and application of dielectric polymers with high permittivity and low energy loss: A mini review." *Journal of Applied Polymer Science* 139, no. 24 (2022): 52367. https://doi.org/10.1002/app.52367

[29] Abdullah, Aziz M., Shujahadeen B. Aziz, M. A. Brza, Salah R. Saeed, Bandar Ali Al-Asbahi, Niyaz M. Sadiq, Abdullah Ahmed Ali Ahmed, and Ary R. Murad. "Glycerol as an efficient plasticizer to increase the DC conductivity and improve the ion transport parameters in biopolymer based electrolytes: XRD, FTIR and EIS studies." *Arabian Journal of Chemistry* 15, no. 6 (2022): 103791. https://doi.org/10.1016/j.arabjc.2022.103791

[30] Shetty, Supriya K., Ismayil, Shreedatta Hegde, V. Ravindrachary, Ganesh Sanjeev, Rajashekhar F. Bhajantri, and Saraswati P. Masti. "Dielectric relaxations and ion transport study of NaCMC: NaNO3 solid polymer electrolyte films." *Ionics* 27 (2021): 2509-2525. https://doi.org/10.1007/s11581-021-04023-y

[31] Ohki, Yoshimichi. "Broadband complex permittivity and electric modulus spectra for dielectric materials research." *IEEJ Transactions on Electrical and Electronic Engineering* 17, no. 7 (2022): 958-972. https://doi.org/10.1002/tee.23565

[32] Rice, M. J., and W. L. Roth. "Ionic transport in super ionic conductors: a theoretical model." *Journal of Solid State Chemistry France* 4, no. 2 (1972): 294-310. https://doi.org/10.1016/0022-4596(72)90121-1

[33] Hu, Liangbing, Chunpeng Yang, Qisheng Wu, Weiqi Xie, Xin Zhang, Jin Zheng, Mounesha Garaga et al. "High-Performance Polymer Ion Conductors Enabled by Decoupled Fast Ions in Molecular Channels." *Nature (Preprint)* (2020). https://doi.org/10.21203/rs.3.rs-114732/v1

[34] Jones, Seamus D., James Bamford, Glenn H. Fredrickson, and Rachel A. Segalman. "Decoupling ion transport and matrix dynamics to make high performance solid polymer electrolytes." *ACS Polymers Au* 2, no. 6 (2022): 430-448. https://doi.org/10.1021/acspolymersau.2c00024